

A

Seminar report

On

## **Medical Mirror**

Submitted in partial fulfillment of the requirement for the award of  
degree  
Of Mechanical

SUBMITTED TO:  
[www.studymafia.org](http://www.studymafia.org)

SUBMITTED BY:  
[www.studymafia.org](http://www.studymafia.org)

## **Acknowledgement**

I would like to thank respected Mr..... and Mr. ....for giving me such a wonderful opportunity to expand my knowledge for my own branch and giving me guidelines to present a seminar report. It helped me a lot to realize of what we study for.

Secondly, I would like to thank my parents who patiently helped me as i went through my work and helped to modify and eliminate some of the irrelevant or un-necessary stuffs.

Thirdly, I would like to thank my friends who helped me to make my work more organized and well-stacked till the end.

Next, I would thank Microsoft for developing such a wonderful tool like MS Word. It helped my work a lot to remain error-free.

Last but clearly not the least, I would thank The Almighty for giving me strength to complete my report on time.

## Preface

I have made this report file on the topic **Medical Mirror**; I have tried my best to elucidate all the relevant detail to the topic to be included in the report. While in the beginning I have tried to give a general view about this topic.

My efforts and wholehearted co-corporation of each and everyone has ended on a successful note. I express my sincere gratitude to .....who assisting me throughout the preparation of this topic. I thank him for providing me the reinforcement, confidence and most importantly the track for the topic whenever I needed it.



## Introduction

Regular and non-invasive assessments of cardiovascular function are important surveillance for cardiovascular catastrophes and treatment therapies of chronic diseases. Resting heart rate, one of the simplest cardiovascular parameters, has been identified as an independent risk factor (comparable with smoking, dyslipidemia or hypertension) for cardiovascular disease [1]. Currently, the gold standard techniques for measurement of the cardiac pulse such as the electrocardiogram (ECG) require patients to wear adhesive gel patches or chest straps that can cause skin irritation and discomfort. Commercial pulseoximetry sensors that attach to the fingertips or earlobes are also inconvenient for patients and the spring-loaded clips can cause pain if worn over a long period of time. The ability to monitor a patient's physiological signals by a remote, non-contact means is a tantalizing prospect that would enhance the delivery of primary healthcare. For example, the idea of performing physiological measurements on the face was first postulated by Pavlidis and associates [2] and later demonstrated through analysis of facial thermal videos. Although non-contact methods may not be able to provide details concerning cardiac electrical conduction that ECG offers, these methods can now enable long-term monitoring of other physiological signals such as heart rate or respiratory rate by acquiring them continuously in an unobtrusive and comfortable manner. Beyond that, such a technology would also minimize the amount of cabling and clutter associated with neonatal ICU monitoring, long-term epilepsy monitoring, burn or trauma patient monitoring, sleep studies, and other cases where a continuous measure of heart-rate is important. The use of photoplethysmography (PPG), a low cost and non-invasive means of sensing the cardiovascular pulse wave (also called the blood volume pulse) through variations in transmitted or reflected light, for non-contact physiological measurements has been investigated recently. This electro-optic technique can provide valuable information about the cardiovascular system such as heart rate, arterial blood oxygen saturation, blood pressure, cardiac output and autonomic function.

Typically, PPG has always been implemented using dedicated light sources (e.g. red and/or infra-red wavelengths), but recent work

has shown that pulse measurements can be acquired using digital camcorders/cameras with normal ambient light as the illumination source. However, all these previous efforts lacked rigorous physiological and mathematical models amenable to computation; they relied instead on manual segmentation and heuristic interpretation of raw images with minimal validation of performance characteristics. Furthermore, PPG is known to be susceptible to motion-induced signal corruption and overcoming motion artifacts presents one of the most challenging problems. In most cases, the noise falls within the same frequency band as the physiological signal of interest, thus rendering linear filtering with fixed cut-off frequencies ineffective. In order to develop a clinically useful technology, there is a need for ancillary functionality such as motion artifacts reduction through efficient and robust image analysis. One technique for noise removal from physiological signals is blind source separation (BSS). BSS refers to the recovery of unobserved signals or 'sources' from a set of observed mixtures with no prior information about mixing process. Typically, the observations are acquired from the output of a set of sensors, where each sensor receives a different combination of the source signals. There are several methods of BSS and in this paper we will focus on BSS by Independent Component Analysis (ICA). ICA is a technique for uncovering the independent source signals from a set of observations that are composed of linear mixtures of the underlying sources. ICA has also been applied to reduce motion artifacts in PPG measurements. In this topic, a novel methodology for non-contact, automated, and motion tolerant cardiac pulse measurements from video images based on blind source separation. Firstly, the approach is described and it is applied to compute heart rate measurements from video images of the human face recorded using a simple webcam. Secondly, we demonstrate how this method can tolerate motion artifacts and validate the accuracy of this approach with an FDA-approved finger blood volume pulse (BVP) measurement device. Thirdly, we show how this method can be easily extended for simultaneous heart rate measurements of multiple persons.

## **Chapter 2**

### **Resting Heart Rate**

Heart rate is the number of heartbeats per unit of time, typically expressed as beats per minute

(bpm) [3]. Heart rate can vary as the body's need to absorb oxygen and excrete carbon dioxide changes, such as during exercise or sleep. The measurement of heart rate is used by medical professionals to

a

assist in the diagnosis and tracking of medical conditions. It is also used by individuals, such as athletes, who are interested in monitoring their heart rate to gain maximum efficiency from their training. The R wave to R wave interval (RR interval) is the inverse of the heart rate.

### **2.1 Measurement of Heart Rate**

Heart rate is measured by finding the pulse of the body. This pulse rate can be measured at any point on the body where the artery's pulsation is transmitted to the surface by pressing it with the index and middle fingers; often it is compressed against an underlying structure like bone. The thumb should not be used for measuring another person's heart rate, as its strong pulse may interfere with discriminating the site of pulsation. Possible points for measuring the heart rate are: 1. The ventral aspect of the wrist on the side of the thumb (radial artery). 2. The ulnar artery. 3. The neck (carotid artery). 4. The inside of the elbow, or under the biceps muscle (brachial artery). 5. The groin (femoral artery). 6. Behind the medial malleolus on the feet (posterior tibial artery). 7. Middle of dorsum of the foot (dorsalis pedis). 8. Behind the knee (popliteal artery). 9. Over the abdomen (abdominal aorta). A more precise method of determining pulse involves the use of an electrocardiograph, or EKG (also abbreviated ECG). Continuous electrocardiograph monitoring of the heart is routinely done in many clinical settings, especially in critical care medicine. Commercial heart rate monitors are also available, consisting of a chest strap with electrodes. The signal is transmitted to a wrist receiver for display. Heart rate monitors allow accurate measurements to be taken continuously and can be used during exercise when manual measurement would be difficult or impossible (such as when the hands are being used).

### **2.2 Measurements at Rest**

The resting heart rate (HR<sub>rest</sub>) is a person's heart rate when they are at rest, that is lying down but awake, and not having recently exerted themselves. The typical healthy resting heart rate in adults is  $60 \pm 80$  bpm, with rates below 60 bpm referred to as bradycardia, and rates above 100 bpm referred to as tachycardia. Note however that conditioned athletes often have resting heart rates below 60 bpm. Cyclist Lance Armstrong had a resting HR around 32 bpm, and it is not unusual for people doing regular exercise to get below 50 bpm. Other cyclists like Miguel Indurain also have a very low heart rate at rest (29 bpm). Musical tempo terms reflect levels relative to resting heart rate; Adagio

(at ease, at rest) is typically  $66 \pm 76$  bpm, similar to human resting heart rate, while Lento

and Largo

("Slow") are  $40 \pm 60$  bpm, which reflects that these tempi are slow relative to normal human heart rate. Similarly, faster tempi correspond to heart rates at higher levels of exertion, such as Andante

(walking:  $76 \pm 108$  bpm) and the like.

The normal heart rate in children is variable and depends on the child's age. The range that should be considered normal are controversial.

## **2.3 Abnormalities**

### **2.3.1 Tachycardia**

Tachycardia is a resting heart rate more than 100 beats per minute. This number can vary as smaller people and children have faster heart rates than average adults.

### **2.3.2 Bradycardia**

Bradycardia is defined as a heart rate less than 60 beats per minute although it is seldom symptomatic until below 50 bpm when a human is at total rest. Trained athletes tend to have slow resting heart rates, and resting bradycardia in athletes should not be considered abnormal if the individual has no symptoms associated with it. For example



Miguel Indurain, a Spanish cyclist and five time Tour de France winner, had a resting heart rate of 29 beats per minute, one of the lowest ever recorded in a healthy human. Again, this number can vary as children and small adults tend to have faster heart rates than average adults.

### **2.3.3 Arrhythmia**

Arrhythmias are abnormalities of the heart rate and rhythm (sometimes felt as palpitations). They can be divided into two broad categories: fast and slow heart rates. Some cause few or minimal symptoms. Others produce more serious symptoms of lightheadedness, dizziness and fainting.

### **2.4 Heart Rate as a Risk Factor**

A number of investigations indicate that faster resting heart rate has emerged as a new risk factor for mortality in homeothermic mammals, particularly cardiovascular mortality in human beings. Faster heart rate may accompany increased production of inflammation molecules and increased production of reactive oxygen species in cardiovascular system, in addition to increased mechanical stress to the heart. There is a correlation between increased resting rate and cardiovascular risk. This is not seen to be "using an allotment of heart beats" but rather an increased risk to the system from the increased rate. An Australian-led international study of patients with cardiovascular disease has shown that heart beat rate is a key indicator for the risk of heart attack. The study, published in

*The Lancet*

(September 2008) studied 11,000 people, across 33 countries, who were being treated for heart problems. Those patients whose heart rate was above 70 beats per minute had significantly higher incidence of heart attacks, hospital admissions and the need for surgery.

## Chapter 3

### Photoplethysmography

#### 3.1 Photoplethysmography

A photoplethysmography [4] (PPG) is an optically obtained plethysmograph, a volumetric measurement of an organ. A PPG is often obtained by using a pulse oximeter which illuminates the skin and measures changes in light absorption. A conventional pulse oximeter monitors the perfusion of blood to the dermis and subcutaneous tissue of the skin. With each cardiac cycle the heart pumps blood to the periphery. Even though this pressure pulse is somewhat damped by the time it reaches the skin, it is enough to distend the arteries and arterioles in the subcutaneous tissue.

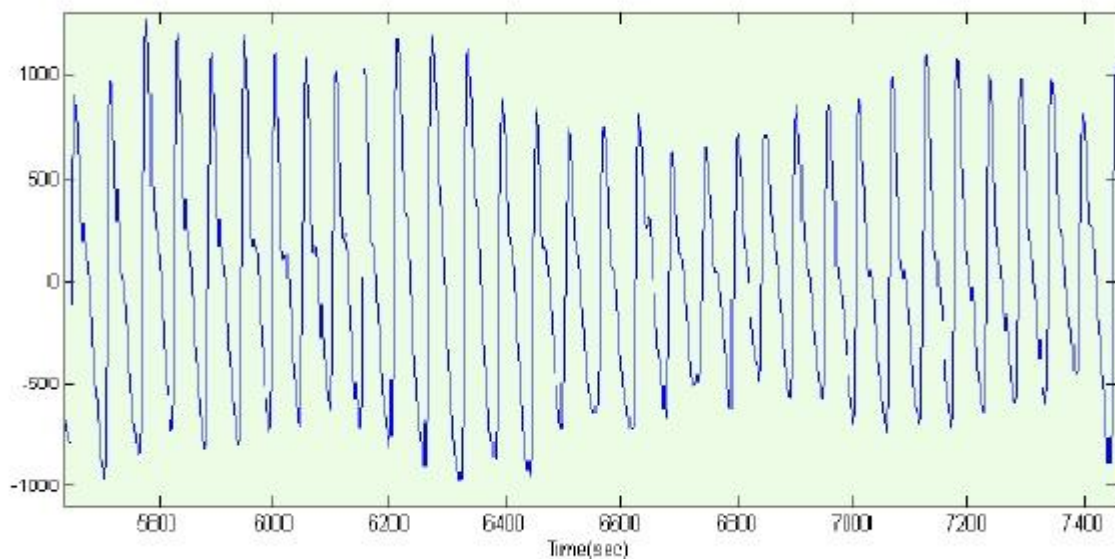


**Figure 3.1** Representative PPG taken from an ear pulse oximeter.

If the pulse oximeter is attached without compressing the skin, a pressure pulse can also be seen from the venous plexus, as a small secondary peak. The change in volume caused by the pressure pulse is detected by illuminating the skin with the light from a light-emitting diode (LED) and then measuring the amount of light either transmitted or reflected to a photodiode. Each cardiac cycle appears as a peak, as seen in the figure. Because bloodflow to the skin can be modulated by multiple other physiological systems, the PPG can also

be used to monitor breathing, hypovolemia, and other circulatory conditions. Additionally, the shape of the PPG waveform differs from subject to subject, and varies with the location and manner in which the pulse oximeter [5] is attached.

### **3.2 Sites for Measuring PPG**

While pulse oximeters are a commonly used medical device the PPG derived from them is rarely displayed, and is nominally only processed to determine heart rate. PPGs can be obtained from transmissive absorption (as at the finger tip) or reflective (as on the forehead). In outpatient settings, pulse oximeters are commonly worn on the finger. However, in cases of shock, hypothermia, etc. blood flow to the periphery can be reduced, resulting in a PPG without a discernible cardiac pulse. In this case, a PPG can be obtained from a pulse oximeter on the head, with the most common sites being the ear, nasal septum, and forehead. PPGs can also be obtained from the vagina and esophagus.

### **3.3 Uses of Photoplethysmography**

#### **3.3.1 Monitoring Heart Rate and Cardiac Cycle**

Because the skin is so richly perfused, it is relatively easy to detect the pulsatile component of the cardiac cycle. The DC component of the signal is attributable to the bulk absorption of the skin tissue, while the AC component is directly attributable to variation in blood volume in the skin caused by the pressure pulse of the cardiac cycle. The height of AC component of the photoplethysmogram is proportional to the pulse pressure, the difference between the systolic and diastolic pressure in the arteries. As seen in the figure showing premature ventricular contractions (PVCs), the PPG pulse for the cardiac cycle with the PVC results in lower amplitude blood pressure and a PPG. Ventricular tachycardia and ventricular fibrillation can also be detected.

#### **3.3.2 Monitoring Respiration**

Respiration affects the cardiac cycle by varying the intrapleural pressure, the pressure between the thoracic wall and the lungs. Since the heart resides in the thoracic cavity between the lungs, the partial pressure of inhaling and exhaling greatly influence the pressure on the vena cava and the filling of the right atrium. This effect is often referred to as normal sinus arrhythmia. During inspiration,

intrapleural pressure decreases by up to 4 mm Hg, which distends the right atrium, allowing for faster filling from the vena cava, increasing ventricular preload, and increasing the stroke volume. Conversely during expiration, the heart is compressed, decreasing cardiac efficiency and reducing stroke volume. However, the overall net effect of respiration is to act as pump for the cardiovascular system. When the frequency and depth of respiration increases, the venous return increases, leading to increased cardiac output.

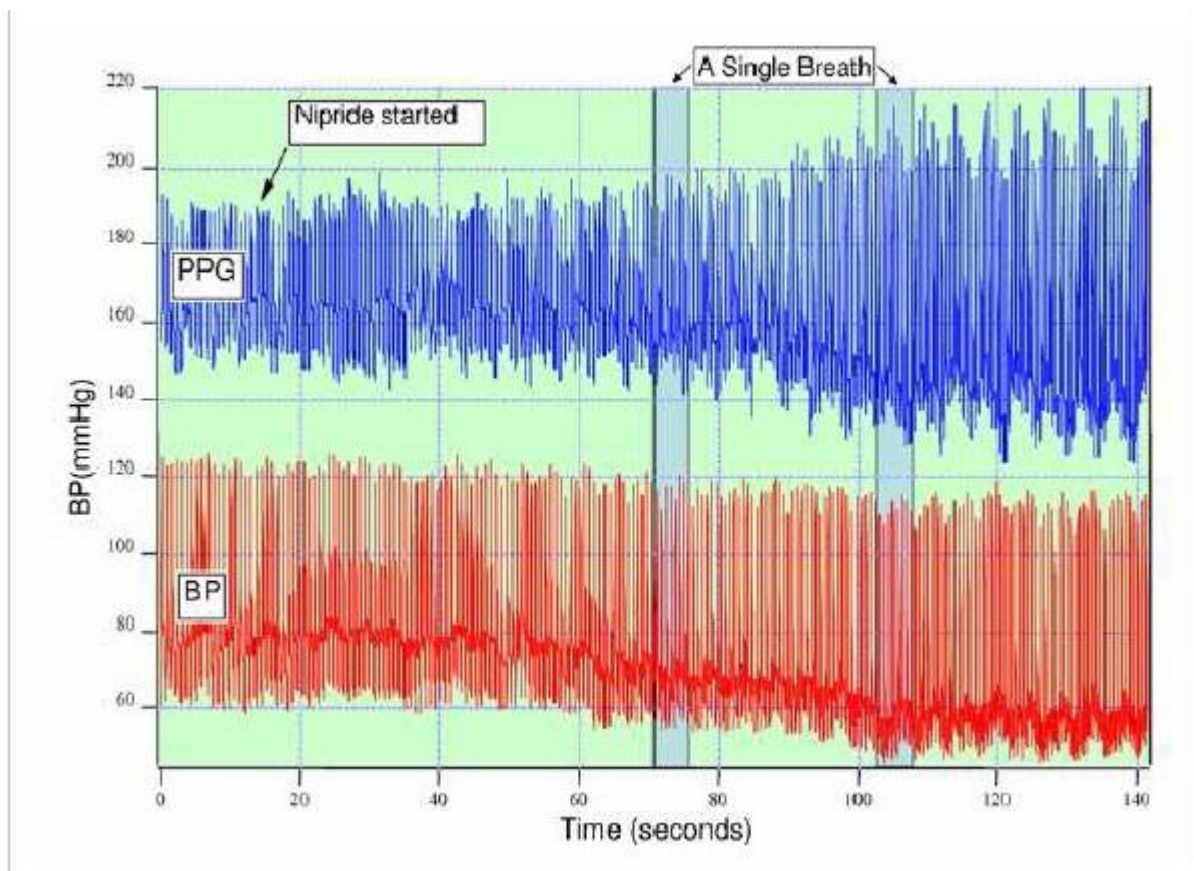


**Figure 3.2** Photoplethysmography of respiration

### 3.3.3 Monitoring Depth of Anesthesia

Anesthesiologist must often judge subjectively whether a patient is sufficiently anesthetized for surgery. As seen in the figure if a patient is not sufficiently anesthetized the sympathetic nervous system response to an incision can generate an immediate response in the amplitude of the PPG.



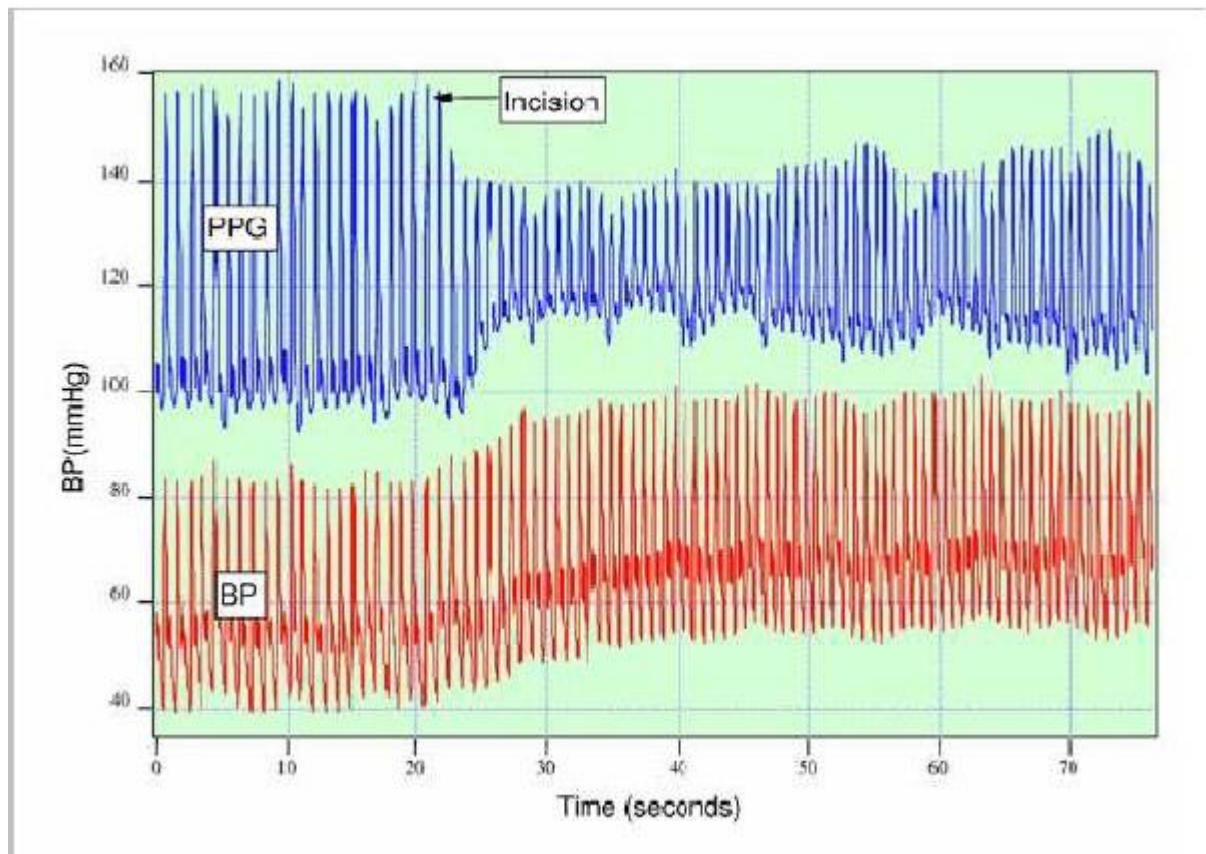


**Figure 3.3** Photoplethysmography under the anesthesia condition

### 3.3.4 Monitoring Hypo and Hypervolemia

Shamir, Eidelman, et al. studied the interaction between inspiration and removal of 10% of a patient's blood volume for blood banking before surgery. They found that blood loss could be detected both from the photoplethysmogram from a pulse oximeter and an arterial catheter. Patients showed a decrease in the cardiac pulse amplitude caused by reduced cardiac preload during exhalation when the heart is being compressed.

## Chapter 4

### Study Description and Experimental Setup

#### 4.1 Experimental setup

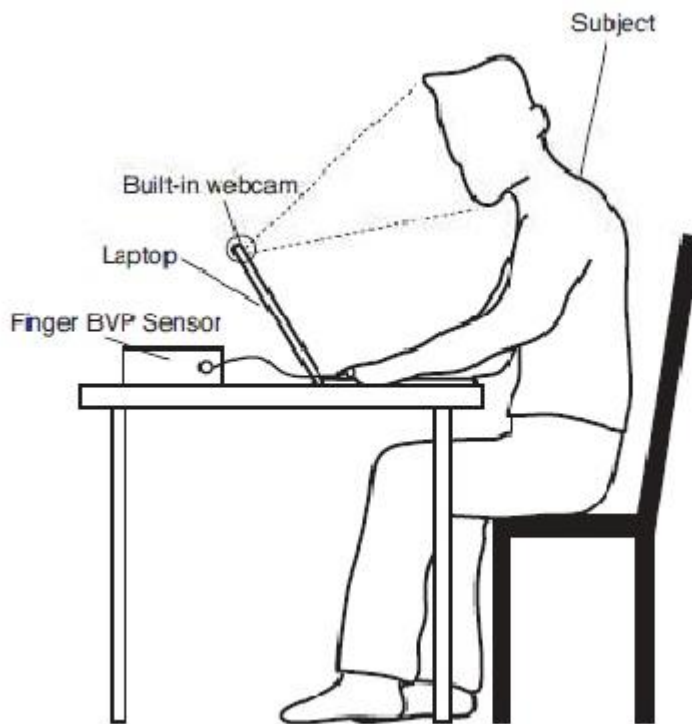


**Figure 4.1** Experimental setup

A basic webcam embedded in a laptop (built-in iSight camera on a Macbook Pro by AppleInc.) was used to record the videos for analysis. All videos were recorded in color (24-bitRGB with 3 channels  $\times$  8 bits/channel) at 15 frames per second (fps) with pixel resolution of  $640 \times 480$  and saved in AVI format on the laptop. 12 participants (10 males, 2 females) between the ages of 18-31 years were enrolled for this study that was approved by theMassachusetts Institute of Technology Committee On the Use of Humans as ExperimentalSubjects (COUHES). The sample featured participants of both genders, different ages andwith varying skin colors (Asians, Africans and Caucasians). Informed consent was obtainedfrom all the participants prior to the start of each study session.

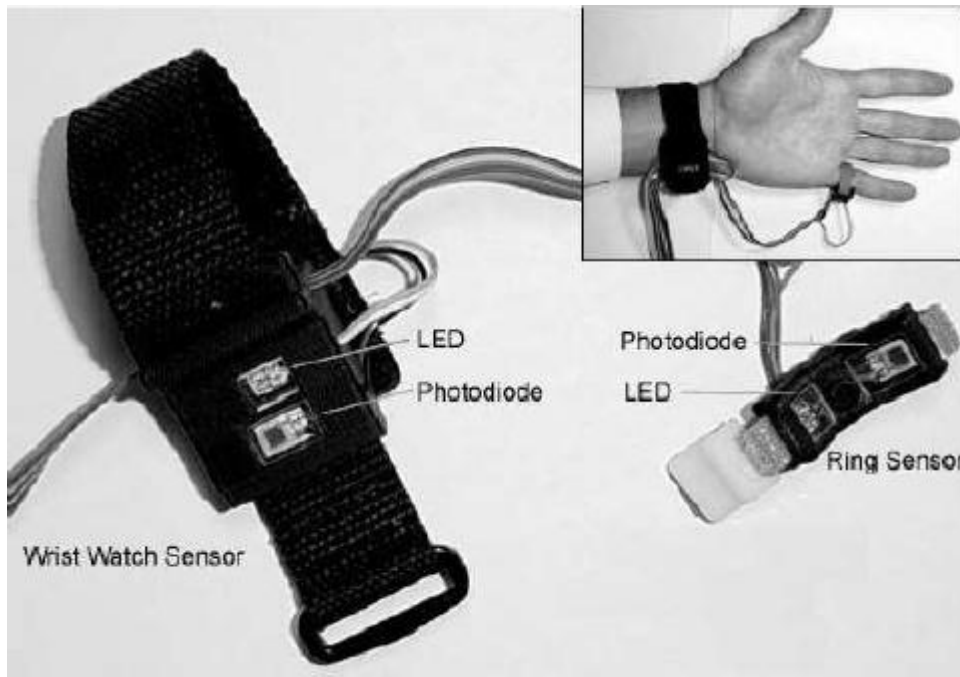


**Figure 4.2** Blood volume pulse sensor

For all experiments, an FDA-approved and commercially available blood volume pulse (BVP) sensor [6] (Flexcomp Infiniti by Thought Technologies Ltd.) was used to measure the participant's BVP signal via a finger probe at 256 Hz for validation. The experiments were conducted indoors and with a varying amount of sunlight as the only source of illumination. Figure 1 shows the experimental setup. Participants were seated at a table in front of a laptop at a distance of approximately 0.5 m from the built-in webcam. Two videos, each lasting one minute, were recorded for all participants. During the first video recording, participants were asked to sit still and stare at the webcam. For the second video recording, participants were asked to move naturally as if they were interacting with the laptop, but to avoid large or rapid motions and to keep the hand wearing the finger BVP sensor still. In addition, single, one-minute video of three participants sitting together at rest was recorded.

## 4.2 Pulse Measurement Methodology

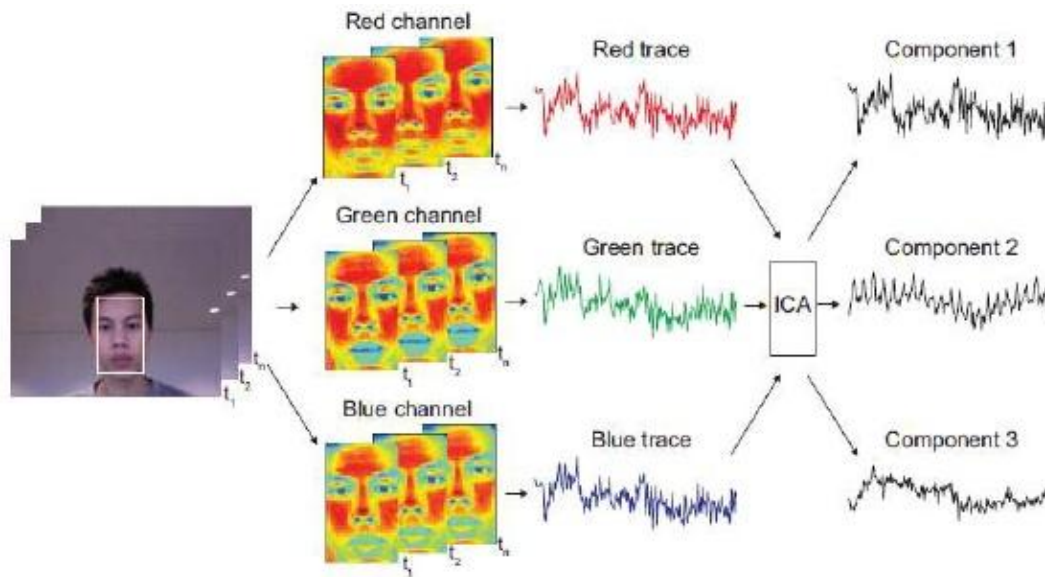


**Figure 4.3** Figure showing the pulse measurement methodology results

Post processing and analysis of both the video and physiological recordings were done using custom software written in MATLAB (The MathWorks, Inc.). First, an automated face tracker was used to detect faces within the video frames and localize the measurement region of interest (ROI) for each video frame. A free MATLAB-compatible version of the OpenComputer Vision (OpenCV) library was used to obtain the coordinates of the face location. The OpenCV face detection algorithm is based on work by Viola and Jones, as well as Lienhart and Maydt. A cascade of boosted classifier uses 14 Haar-like digital image features trained with positive and negative examples. The pre-trained frontal face classifier available with OpenCV 2.0 was used. The cascade nature uses a set of simple classifiers that are applied to each area of interest sequentially. At each stage a classifier is built using a weighted vote, known as boosting. Either all stages are passed, meaning the region is likely to contain a face, or the area is rejected. The dimensions of the area of interest are changed sequentially in order to identify positive matches of different sizes. For each face detected, the algorithm returns the x- and y-coordinates along with the



height and width that define a box around the face. From this output, the centre 60% width and full height of the box was selected as the ROI for subsequent calculations. To prevent face segmentation errors [7] from affecting the performance of our algorithm, the face coordinates from the previous frame were used if no faces were detected. If multiple faces were detected when only one was expected, then our algorithm selected the face coordinates that were the closest to the coordinates from the previous frame.

The ROI was then separated into the three RGB channels and spatially averaged over all pixels in the ROI to yield a red, blue and green measurement point for each frame and form the raw traces

$x_1(t)$ ,  $x_2(t)$  and  $x_3(t)$  respectively.. Subsequent processing was performed using a 30 s moving window with 96.7% overlap (1 s increment). The raw RGB traces are normalized as follows:

$$x(t) - \frac{X_i(t)\mu_i}{\sigma_i}$$

for each  $i = 1, 2, 3$  where  $i$ ,  $\mu$  and  $\sigma$  are the mean and standard deviation of  $x_i(t)$  respectively. The normalization transforms  $x_i(t)$  to  $x_i'(t)$  which is zero-mean and has unit variance.

### 4.3 Mean

Mean is where you add up all the numbers and divide it by the amount of numbers there were. There are other statistical measures that use samples that some people confuse with averages - including 'median' and 'mode'. Other simple statistical analyses use measures of spread, such as range, inter quartile range, or standard deviation. For a real-valued random variable  $X$ , the mean is the expectation of  $X$ . For a data set, the mean is the sum of the values divided by the number of values. The mean of a set of numbers  $x_1, x_2, \dots, x_n$  is typically denoted by  $\bar{x}$ , pronounced "x bar". This mean is a type of arithmetic mean. If the data set was based on a series of observations obtained by sampling a statistical population, this mean is termed the "sample mean" to distinguish it from the "population mean". The mean of an image is the mean values of gray level values of all its pixels. The mean is given by the formulae

$$u = (r * c)^{-1} \sum_{i=1}^r \sum_{j=1}^c F(i, j)$$

Where,  $u$ =mean

$F(i,j)$ =the image frame

$r$  =number of rows of the image

$c$ =number of columns of the image

#### 4.4 Standard Deviation

Standard deviation is a widely used measurement of variability or diversity used in statistics and probability theory. It shows how much variation or "dispersion" there is from the "average" (mean, or expected/budgeted value). A low standard deviation indicates that the data points tend to be very close to the mean, whereas high standard deviation indicates that the data are spread out over a large range of values. Technically, the standard deviation of a statistical population, data set, or probability distribution is the square root of its variance. It is algebraically simpler though practically less robust than the average absolute deviation. A useful property of standard deviation is that, unlike variance, it is expressed in the same units as the data. Note, however, that for measurements with percentage as unit, the standard deviation will have percentage points as unit.

The standard deviation of a 2-D image is calculated for all the pixel values of the image. It is given by the formulae

$$\sigma = \sqrt{(r * c)^{-1} \sum_{i=1}^r \sum_{j=1}^c (F(i, j) - u)^2}$$

Where,  $\sigma$  =standard deviation

$u$ =mean value of the image.

$F(i,j)$ =the image frame.

$r$  =number of rows of the image.

$c$ =number of columns of the image.

## **Chapter 5 Blind Signal Separation and FFT**

### **5.1 Blind Source Separation**

The technique used for noise removal from physiological signals is blind source separation (BSS) [8]. Typically, the observations are acquired from the output of a set of sensors, where each sensor receives a different combination of the source signals. Blind signal separation, also known as blind source separation, is the separation of a set of signals from a set of mixed signals, without the aid of information (or with very little information) about the source signals or the mixing process. Blind signal separation relies on the assumption that the source signals do not correlate with each other. For example, the signals may be mutually statistically independent or decorrelated. Blind signal separation thus separates a set of signals into a set of other signals, such that the regularity of each resulting signal is maximized, and the regularity between the signals is minimized i.e. statistical independence is maximized. Because temporal redundancies (statistical regularities in the time domain) are "clumped" in this way into the resulting signals, the resulting signals can be more effectively deconvolved than the original signals. There are different methods of blind signal separation:

- Principal components analysis
- Singular value decomposition
- Independent component analysis
- Dependent component analysis
- Non-negative matrix factorization
- Low-Complexity Coding and Decoding
- Stationary Subspace Analysis

Here we will focus on BSS by Independent Component Analysis

The normalized raw traces are then decomposed into three independent source signals using ICA [9]. In this report, we used the joint approximate diagonalization of eigen matrices (JADE) algorithm developed by Cardoso. This approach by tensorial methods uses fourth-order cumulant tensors and involves the joint diagonalization of cumulant matrices; the solution of this approximates statistical independence of the sources (to the fourth order). Although there is no ordering of the ICA components, the second component typically contained a strong

plethysmographic signal. For the sake of simplicity and automation, the second component was selected as the desired source signal.

## 5.2 Independent Component Analysis

Independent component analysis (ICA) is a computational method for separating a multivariate signal into additive subcomponents supposing the mutual statistical independence of the non-Gaussian source signals. It is a special case of blind source separation.

When the independence assumption is correct, blind ICA separation of a mixed signal gives very good results. It is also used for signals that are not supposed to be generated by a mixing for analysis purposes. A simple application of ICA is the 'cocktail party problem', where the underlying speech signals are separated from a sample data consisting of people talking simultaneously in a room. Usually the problem is simplified by assuming no time delays or echoes. An important note to consider is that if  $N$  sources are present, at least  $N$  observations (e.g. microphones) are needed to get the original signals. This constitutes the square ( $J = D$ , where  $D$  is the input dimension of the data and  $J$  is the dimension of the model). Other cases of underdetermined ( $J < D$ ) and over determined ( $J > D$ ) have been investigated. ICA finds the independent components (aka factors, latent variables or sources) by maximizing the statistical independence of the estimated components. We may choose one of many ways to define independence, and this choice governs the form of the ICA algorithms. The two broadest definitions of independence for ICA are

- 1) Minimization of Mutual Information
- 2) Maximization of non-Gaussianity



The Non-Gaussianity family of ICA algorithms, motivated by the central limit theorem, uses kurtosis and negentropy. The Minimization-of-Mutual information (MMI) family of ICA algorithms uses measures like Kullback-Leibler Divergence and maximum-entropy. Typical algorithms for ICA use centering, whitening (usually with the eigenvalue decomposition), and dimensionality reduction as preprocessing steps in order to simplify and reduce the complexity of the problem for the actual iterative algorithm. Whitening and dimension reduction can be achieved with principal component analysis or singular value decomposition. Whitening ensures that all dimensions are treated equally *a priori* before the algorithm is run. Algorithms for ICA include infomax, FastICA, and JADE, but there are many others also. In general, ICA cannot identify the actual number of source signals, a uniquely correct ordering of the source signals, nor the proper scaling (including sign) of the source signals. ICA is important to blind signal separation and has many practical applications. It is closely related to (or even a special case of) the search for a factorial code of the data, i.e., a new vector-valued representation of each data vector such that it gets uniquely encoded by the resulting code vector (loss-free coding), but the code components are statistically independent.

### 5.2.1 Mathematical Definitions

Linear independent component analysis can be divided into noiseless and noisy cases, where noiseless ICA is a special case of noisy ICA. Nonlinear ICA should be considered as a separate case.

The data is represented by the random vector  $\mathbf{x}=(x_1, \dots, x_m)$  and the components as the random vector  $\mathbf{s}=(s_1, \dots, s_m)$ . The task is to transform the observed data, using a linear static transformation

$\mathbf{W}$  as  $\mathbf{s}=\mathbf{W}\mathbf{x}$ , into maximally independent components

$\mathbf{S}$  measured by some function  $F(s_1, \dots, s_m)$  of independence.

### Linear Noiseless ICA

The components

錚

砵  
倩

of the observed random vector

鉶  
冇  
浼

鉶

菰

塱 茌 茌 塱

鉶

冇

菰倩

塱

are generated as asum of the independent components

鉶

冇

,

**$k=1,.....,n:$**

鉶

砵

冇 瀟

砵塱菰

鉶

菰

+

倩 茌 茌 佞 佞 後 倩

瀟

砵塱

冇

鉶

冇

後 倩 茌 茌 佞 後 倩

瀟

砵堧倅  
 鉀  
 倅

weighted by the mixing weights

倅  
 堧  
 砵堧  
 有

•

### Linear Noisy ICA

With the added assumption of zero-mean and uncorrelated Gaussian noise  $n$ , the ICA model takes the form

$$x = As + n$$

### Identifiability

The independent components are identifiable up to a permutation and scaling of the sources. This identifiability [10] requires that:

At most one of the sources 鉀有 is Gaussian,

‡ The number of observed mixtures  $m$ , must be at least as large as the number of estimated components  $n$ :  $m \geq n$ . It is equivalent to say that the mixing matrix  $A$  must be of full rank for its inverse to exist.

In this study, the underlying source signal of interest is the cardiovascular pulse wave that propagates throughout the body. Volumetric changes in the facial blood vessels during the cardiac cycle modify the path length of the incident ambient light such that the subsequent changes in amount of reflected light indicate the timing of cardiovascular events. By recording a video of the facial region with a webcam, the RGB color sensors pick up a mixture of the reflected plethysmographic signal along with other sources of fluctuations in light due to artifacts such as motion and changes in ambient lighting conditions. Given that hemoglobin absorptivity differs across the visible and near-infrared spectral range, each color sensor records a mixture of the original source signals with slightly different weights. These observed signals from the red, green and blue color sensors are denoted by 倅有鉀( $t$ ), 有紃( $t$ ) and 有堧( $t$ ) respectively, which are amplitudes of the recorded signals (averages of all pixels in



the facial region) at time point  $t$ . In conventional ICA the number of recoverable sources cannot exceed the number of observations, thus we assumed three underlying source signals, represented by  $\mathbf{x}_1(t)$ ,  $\mathbf{x}_2(t)$  and  $\mathbf{x}_3(t)$ . The ICA model assumes that the observed signals are linear mixtures of the sources, i.e.  $\mathbf{x}(t) = \mathbf{A}\mathbf{s}(t)$  for each  $i = 1, 2, 3$

for each  $i = 1, 2, 3$

This can be represented compactly by the mixing equation

$$\mathbf{x}(t) = \mathbf{A}\mathbf{s}(t)$$

The column vectors  $\mathbf{s}_1(t)$ ,  $\mathbf{s}_2(t)$  and  $\mathbf{s}_3(t)$  are the source signals. The square  $3 \times 3$  matrix  $\mathbf{A}$  contains the mixture coefficients  $a_{ij}$ . The aim of ICA is to find a separating or demixing matrix that is an approximation of the inverse of the original mixing matrix  $\mathbf{A}$  whose output

$$\hat{\mathbf{s}}(t) = \mathbf{W}\mathbf{x}(t)$$

is an estimate of the vector  $\mathbf{s}(t)$  containing the underlying source signals. According to the central limit theorem [11], a sum of independent random variables is more Gaussian than the original variables. Thus, to uncover the independent sources,  $\mathbf{W}$  must maximize the non-Gaussianity of each source. In practice, iterative methods are used to maximize or minimize a given cost function that measures non-Gaussianity such as kurtosis, negentropy or mutual information.

finally we applied the fast Fourier transform (FFT) on the selected source signal to obtain the power spectrum. The pulse frequency was designated as the frequency that corresponded to the highest power of the spectrum within an operational frequency band. We set the operational range to [0.75, 4] Hz (corresponding to [45, 240] bpm) to provide a wide range of heart rate measurements. Similarly, we obtained the reference heart rate measurements from the recorded finger BVP signal.

### 5.3 FFT

A fast Fourier transform (FFT) is an efficient algorithm to compute the discrete Fourier transform (DFT) and its inverse. There are many distinct FFT algorithms involving a wide range of mathematics, from simple complex-number arithmetic to group theory and number theory. A DFT decomposes a sequence of values into



components of different frequencies. This operation is useful in many fields (see discrete Fourier transform for properties and applications of the transform) but computing it directly from the definition is often too slow to be practical. An FFT is a way to compute the same result more quickly.

Computing a DFT of  $N$  points in the naive way, using the definition, takes  $O(N^2)$  arithmetical operations, while an FFT can compute the same result in only  $O(N \log N)$  operations. The difference in speed can be substantial, especially for long data sets where  $N$  may be in the thousands or millions<sup>2</sup> in practice, the computation time can be reduced by several orders of magnitude in such cases, and the improvement is roughly proportional to  $N / \log(N)$ . This huge improvement made many DFT-based algorithms practical; FFTs are of great importance to a wide variety of applications, from digital signal processing and solving partial differential equations to algorithms for quick multiplication of large integers.

The most well known FFT algorithms depend upon the factorization of  $N$ , but (contrary to popular misconception) there are FFTs with  $O(N \log N)$  complexity for all  $N$ , even for prime  $N$ . Many FFT algorithms only depend on the fact that  $\omega_N$  is a primitive root of unity, and thus can be applied to analogous transforms over any finite field, such as number-theoretic transforms. Since the inverse DFT is the same as the DFT, but with the opposite sign in the exponent and a  $1/N$  factor, any FFT algorithm can easily be adapted for it. An FFT computes the DFT and produces exactly the same result as evaluating the DFT definition directly; the only difference is that an FFT is much faster. (In the presence of round-off error, many FFT algorithms are also much more accurate than evaluating the DFT definition directly, as discussed below.) Let  $x_0, \dots, x_{N-1}$  be complex numbers. The DFT is defined by the formula

有  
有  
有  
油  
鉅

俵修符菰俵杆璦  
 俵  
 符砵倭倭倭倭  
 有  
 洩俵健修菰

Evaluating this definition directly requires  $O(N^2)$  operations, there are  $N$  outputs  $X_k$ , and each output requires a sum of  $N$  terms. An FFT is any method to compute the same results in  $O(N \log N)$  operations. More precisely, all known FFT algorithms require  $O(N \log N)$  operations (technically,  $O$  only denotes an upper bound), although there is no proof that better complexity is impossible. To illustrate the savings of an FFT, consider the count of complex multiplications and additions. Evaluating the DFT's sums directly involves  $N^2$  complex multiplications and  $N(N-1)$  complex additions [of which  $O(N)$  operations can be saved by eliminating trivial operations such as multiplications by 1. The well-known radix-2 Cooley-Tukey algorithm, for  $N$  a power of 2, can compute the same result with only  $(N/2) \log_2 N$  complex multiplies (again, ignoring simplifications of multiplications by 1 and similar) and  $N \log_2 N$  complex additions. In practice, actual performance on modern computers is usually dominated by factors other than arithmetic and is a complicated subject, but the overall improvement from  $O(N^2)$  to  $O(N \log N)$  remains.

#### 5.4 Threshold BPM Selection

Despite the application of ICA in our proposed methodology, the pulse frequency computation may occasionally be affected by noise [12]. To address this issue, we utilize the historical estimations of the pulse frequency to reject artifacts by fixing a threshold for maximum change in pulse rate between successive measurements (taken 1 s apart). If the difference between the current pulse rate estimation and the last computed value exceeded the threshold (we used a threshold of 12 bpm in our experiments), the algorithm rejected it and searched the operational frequency range for the frequency corresponding to the next highest power that met this constraint. If no frequency peaks that met the criteria were located, then the algorithm retained the current pulse frequency estimation.

## **Chapter 6**

### **Results**

#### **Figure 6.1**

A person standing before the camera embedded mirror

WWW.STUDYMAFIA.ORG



G trace



R trace



B trace

**Figure 6.2**

Figure showing the raw traces



**Figure 6.7**

Mirror showing the heart beat of the person

### **Conclusions and Future Scope**

This concept describes a novel methodology for recovering the cardiac pulse rate from videorecordings of the human face and implementation using a simple webcam with ambient daylight providing illumination. This is the first demonstration of a low-cost method for non-contact heart rate measurements that is automated and motion-tolerant. Moreover, this approach is easily scalable for simultaneous assessment of multiple people in front of a camera. Given the low cost and widespread availability of webcams, this technology is promising for extending and improving access to medical care.

Although this concept only addressed the recovery of the cardiac pulse rate, many other important physiological parameters such as respiratory rate, heart rate variability and arterial blood oxygen saturation can potentially be estimated using the proposed technique. Creating a real-time, multi parameter physiological measurement platform based on this technology will be the subject of future work.

## Reference

- [www.google.com](http://www.google.com)
- [www.wikipedia.com](http://www.wikipedia.com)
- [www.studymafia.org](http://www.studymafia.org)
- [www.pptplanet.com](http://www.pptplanet.com)

www.studymafia.org